J Mater Sci (2009) 44:6155–6161
DOI 10.1007/s10853-009-3851-7

Mechanical behavior of Au–In intermetallics for low temperature solder diffusion bonding

Jie Lian · Steven Jan Wo Chun · Mark S. Goorsky · Junlan Wang

Received: 26 May 2009 / Accepted: 26 August 2009 / Published online: 10 September 2009

Abstract In this study, gold (Au)–indium (In) intermetallic compounds (IMCs) formation for low temperature solder bonding was investigated by imbedding a gold wire into the annealing indium solder. According to available research on liquid–solid reaction of gold and indium, experiments were only conducted at an annealing temperature in the range of 200–300 °C. To investigate the feasibility of forming the Au–In IMCs at lower temperature, a low annealing temperature of 160 °C was applied in this study, which is just above the melting point of indium of 156 °C. $AuIn_2$ precipitates were confirmed to be predominately formed in the IMCs by X-ray diffraction. Different annealing times of 10, 40, and 120 min were applied to study the stabilization time of IMC $AuIn_2$. With thermal considerations, $AuIn_2$ was confirmed to form with a low annealing temperature of 160 °C, and a short annealing time of 10 min. In addition, the microstructure of the cross-sections in the interfacial region of the gold wire and indium solder was investigated by scanning electron microscopy. The mechanical behavior of gold, indium, and their IMCs with different annealing times were studied by nanoindentation. Mechanical properties including reduced modulus and hardness were extracted after taking into account of the pile-up effect. Increased reduced modulus and hardness were observed with increasing annealing times, due to the strengthening of the atomic bonding in the compounds. The reduced modulus and hardness measured from nanoindentation indicate a significant strengthening of the indium solder by the $AuIn_2$ nanoparticles.

J. Lian · J. Wang (✉)
Department of Mechanical Engineering, University of Washington, Seattle, WA 98195, USA
e-mail: junlan@u.washington.edu

S. J. W. Chun · M. S. Goorsky
Department of Materials Science, University of California, Los Angeles, CA 90095, USA

Introduction

Three-dimensional integration of circuit chips and wafers plays an important role in structuring highly miniaturized and complex detector systems. Different processing technologies including thin-film technology, micromachining, microbumping, wafer thinning, and advanced assembly have been widely developed to enhance the integration quality and reliability [1]. Among these processing technologies, flip chip solder interconnect technology has become an attractive first level interconnect solution due to its high packaging density, miniaturized feature, and good thermal and electrical performance [2–4]. Solder diffusion bonding, where two elements react to form an intermetallic compound (IMC), is an important process involved in the flip chip technology. For example, under-bump metallurgy (UBM) utilizes the metallic pad to place solder bumps at the desired location, and provides electrical, thermal, and mechanical linkages between two metallic surfaces [5].

During the flip chip solder interconnect process, the reliability issues are always crucial considerations in the electronic packing, as degradation or failure in interlayers will significantly affect products function, especially in their thermal and mechanical properties [2]. While high temperature bonding could degrade chip performance, solder diffusion bonding process with low temperature (<350 °C) can potentially solve the issues of heat sensitive components and structures [6]. On the other hand, the mechanical properties of intermetallic reaction layers become especially important for portable products, which frequently experience mechanical shock loadings caused

by dropping of devices [7]. Moreover, the IMCs in the solder is typically less than several microns in size and is inclined to form cracks and voids causing a reduced load-carrying capacity and loss of conductivity. From the above reliability considerations, it is important to study the IMCs mechanical behavior after elevated temperature annealing, and it is desirable to develop a low temperature bonding structure with high enough strength.

In this study, based on the thermal and mechanical considerations, indium and gold were chosen for the low temperature solder diffusion bonding. Indium solders with a low melting temperature have the advantage of high oxidation-resistance, and high electrical and thermal conductivities, and usually serve as a wetting layer in UBM process. Gold serves as a good protective layer in UBM [5]. In this study, Au–In low temperature IMCs formation was investigated by imbedding a gold wire into the annealing indium solder. The microstructure of gold, indium, and their IMCs were studied by XRD and SEM, while their mechanical behavior was studied by nanoindentation.

Experimental methods

In the interdiffusion of gold and indium for solid–solid state reactions at room temperature, four different IMCs of Au–In were reported to form as $AuIn_2$, AuIn, Au_7In_3, and Au_4In [8]. However, several researches have reported that when annealing temperature ranging from 200 to 300 °C was applied, only $AuIn_2$ was formed in the IMCs [5, 9–11]. In this study, in order to study low temperature diffusion bonding and the formation of $AuIn_2$, an annealing temperature of 160 °C was chosen, which is right above the indium melting point of ~156 °C but lower than the available data at 200 °C in literature.

In many studies on solder diffusion bonding in UBM, the packing of multilayers of thin films are fabricated in the series of protection layer/wetting layer/adhesion layer. Recent studies on mechanical characterization of intermetallic layers by nanoindentation have been reported [12–14]. In the Au–In based multilayer structure in UBM, gold acts as oxidation protective layer and top surface metallurgy, indium acts as the wetting layer, and other metals such as titanium, copper can serve as the adhesion layer [5]. The adhesion layers could react with Au–In intermetallic with low temperature annealing, and form new IMCs besides Au–In intermetallic. In this study, instead of creating multilayer structures, a gold wire was imbedded into the indium solder to form dissolution of gold into indium. In this way, only Au–In intermetallics were produced for investigation. Then microstructural and mechanical characterizations were performed on the flat cross-sectional surface across the gold circular cross-section, the Au–In IMCs and the bulk indium region.

Sample preparation

With both the temperature and structure considerations, three samples of the gold wire imbedded indium compounds were prepared with different annealing times. First, three vials with identical amounts of indium pellets were placed on a hotplate with temperature set to 160 °C. Once the indium was melted, a gold wire was submerged into the liquid indium in each vial, and held for 10, 40, and 120 min, respectively, to anneal the compound. This is expected to produce a reaction between the gold and indium to form the intermetallic $AuIn_2$. Different annealing times were applied to study the stabilization time of $AuIn_2$. After annealing, the samples were set aside from the hotplate to cool down. The samples were then mechanically polished with silicon carbide sandpaper down to 1,200 grit. Because indium is extremely soft and the silicon carbide particles can be easily embedded in the indium during the polishing, long time polishing could contaminate the indium surface [15]. In the study of bonding gold thin films with indium solder, So and Lee [16] found that the softer indium was polished away, and the IMCs were concentrated on the cross-sectional surface of Au–In bi-layers. In this study, in order to avoid the severe contamination of indium, mechanical polishing was performed for a very short time. The roughness effect on mechanical properties is expected to be much less than the effect from imbedding more of the hard silicon carbide particles.

Experimental techniques

The microstructure of the cross-sections of the gold wire and indium solder was characterized by SEM (XL30 FEG). All samples were imaged with a 15 kV accelerating potential with magnifications ranging from 250 to 500×.

The composition in the interfacial region of gold wire and indium solder was determined by X-ray diffraction (XRD). A Bruker AXS D8 advanced X-ray diffractometer with Cu $K_{\alpha 1}$ implement radiation was used for XRD measurement. The X-ray wavelength is 1.54060 Å for Cu $K_{\alpha 1}$. All scans were taken in continuous mode for a 2θ range of 0–60°.

Nanoindentation tests were carried out on interfacial regions of the gold wire and indium solder by using a Ubi1 nanomechanical test instrument (Hysitron, Inc., MN). A three-sided diamond pyramidal cube corner tip with a nominal radius of curvature around 50 nm was used as the indenter tip. The load and displacement were continuously monitored by a three-plate capacitive force/displacement transducer. Reduced modulus and hardness were

determined from the load–displacement information following the procedure developed by Oliver and Pharr [17]. The hardness (H) is defined as the ratio of the maximum indentation load P_{max} over the contact area A_c:

$$H = \frac{P_{max}}{A_c}, \quad (1)$$

and the reduced modulus E_r is calculated by:

$$E_r = \frac{\sqrt{\pi}}{2\sqrt{A_c}}S, \quad (2)$$

where S is the measured contact stiffness at initial unloading, and A_c is the contact area. The contact area as a function of contact depth is calibrated by indenting on a fused quartz standard. The reduced modulus is a property that accounts for elastic deformations in both the material being indented and the indenter and is defined by:

$$\frac{1}{E_r} = \frac{1-\nu_i^2}{E_i} + \frac{1-\nu_s^2}{E_s}, \quad (3)$$

where ν_i and E_i are the Poisson's ratio and Young's modulus of the indenter, and ν_s and E_s are the Poisson's ratio and Young's modulus of the sample. The indenter tip is made of diamond with a Poisson's ratio and Young's modulus of 0.07 and 1140 GPa, respectively. Thus, the Young's modulus of the sample is directly dependent on the reduced modulus.

Experimental results

Microstructure

The microstructure of the cross-sections of the gold wire and indium solder and the IMCs was investigated by SEM. Figure 1a shows the SEM image of the polished Au wire–In solder sample, which was annealed at 160 °C for 40 min. In the SEM image, the color contrast reflects the surface topography. Based on the process of imbedding the gold wire into the indium solder, it can be clearly differentiated that the Au wire centers in the bright circle, and the annealed indium is the dark region outside the bright circle. Figure 1b points out different possible compositions of the material. As indium is extremely soft, the silicon carbide (SiC) particles can be easily embedded in the indium during polishing. Therefore, the darkest parts of the image could be the embedded SiC particles and the gray region could be the Au/In IMC. Further confirmation of the composition in the interfacial region was obtained by conducting XRD and nanoindentation in the different regions. Figure 2 shows the XRD graph in all three samples annealed at 160 °C for 10, 40, and 120 min, respectively. It confirms that there exists IMCs in the interfacial region, and the compounds are only in the form of $AuIn_2$, other than AuIn, Au_7In_3, or Au_4In, which are usually

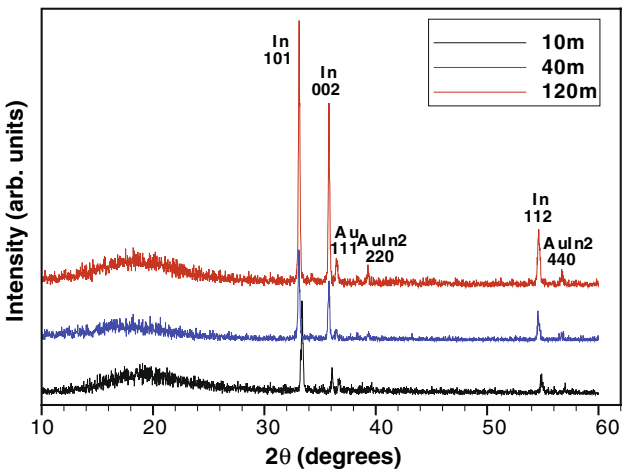

Fig. 2 XRD graph of the Au wire–In solder structure

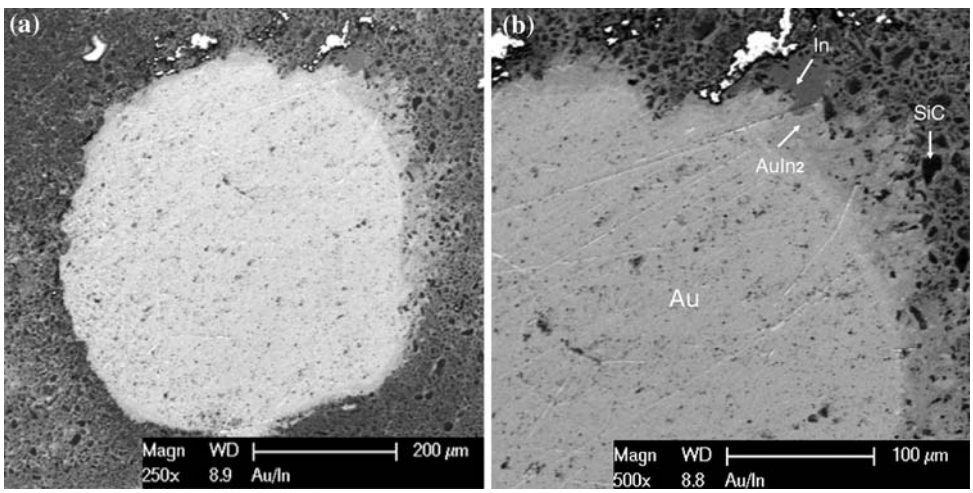

Fig. 1 SEM image of: **a** Au wire–In solder sample; **b** different particles could reside in the interfacial region of Au wire–In solder

formed at room temperature. Thus, it can be concluded that $AuIn_2$ can be formed at a low annealing temperature of 160 °C with an annealing time ranging from 10–120 min.

Mechanical behavior

According to the SEM imaging of the sample topography and the XRD analysis of the sample composition, the cross-sections of the gold wire and indium solder are composed of gold, indium, and their IMC $AuIn_2$. In order to characterize the mechanical properties, nanoindentation was performed on the Au wire–In solder samples with annealing times of 10, 40, and 120 min. Figure 3 shows the scanning probe microscopy image of different indentation spots across the interfacial region of the gold wire and indium solder annealed at 160 °C for 40 min. A series of indents were performed across the gold wire and indium solder interfacial region, and thus different load–displacement responses and mechanical properties can be extracted and compared. Based on the distinctly different load–displacement behavior and the measured mechanical properties, different composition of gold, indium, and $AuIn_2$ can be confirmed. Figure 4 compares the load–displacement responses in gold, indium, and $AuIn_2$ for samples of three different annealing times. Apparently, the load–displacement response in indium is more compliant than that of gold and $AuIn_2$. With the same maximum indentation load, the maximum indentation depth in indium is much higher than that in $AuIn_2$ and gold. This indicates a much lower hardness in indium than $AuIn_2$ and gold. Upon unloading, indium recovers 98 nm of the total 570 nm indentation depth, which corresponds to an elastic recovery of 17.2%. The elastic recovery is 14.9% for $AuIn_2$ annealed for 10 min, 18.8% for $AuIn_2$ annealed for 40 min, and 19.8% for $AuIn_2$ annealed for 120 min. For unloading of gold, the

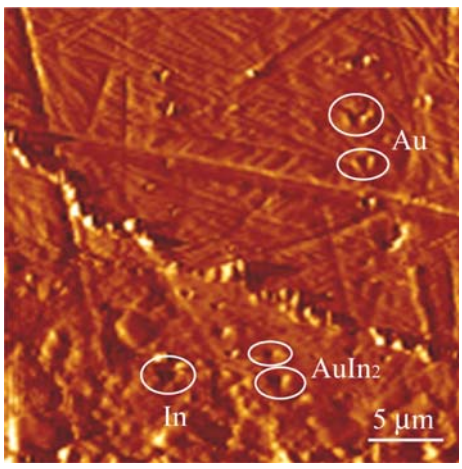

Fig. 3 Scanning probe microscopy image of different indentations across the interfacial region of Au and In for the Au wire–In solder annealed at 160 °C for 40 min

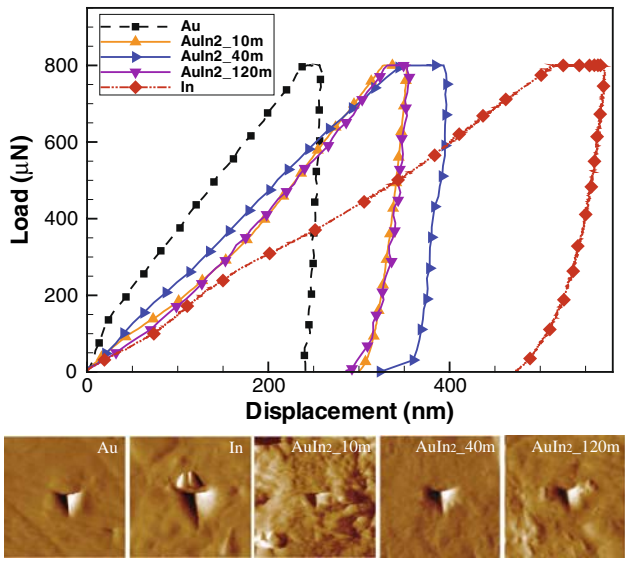

Fig. 4 Load–displacement response of nanoindentation on Au, In, and the IMC $AuIn_2$ for three Au wire–In solder samples annealed at 160 °C for 10, 40, and 120 min, respectively, and the scanning probe microscopy images with area of 5 × 5 μm of each nanoindentation

elastic recovery is only 8%. Thus, gold has the lowest degree of elastic recovery.

Mechanical properties and pile-up effect

For nanoindentation on some soft materials, there is limited elasticity to accommodate the volume of the indenter by plastic flow. Materials volume is pushed out to the sides of the indenter to form a pile-up. The pile-up effect can lead to inaccurate characterization of elastic modulus and hardness due to underestimation of the projected contact area, thus it is important to correct the contact area when pile-up effect is prominent. Pile-up around the indent was observed in this study from the indentation images of gold, indium, and the intermetallic $AuIn_2$. Figure 5 shows the scan line profile of each indent on the three materials. Li and Bhushan [18] stated that the Oliver–Pharr method can underestimate the true contact area by as much as 50% for soft materials and high loads. Thus, with maximum indentation load up to 1000 μN, the contact area should be corrected in this study. Kese et al. [19] proposed a simple semi-ellipse model to modify the contact area for Berkovich indenter tip. In the model, the pile-up area on each side of the equilateral triangle indent was considered as a semi-ellipse, and the total pile-up area was summed over the three side areas as:

$$A_{PU} = \frac{\pi l}{4} \sum a_i, \tag{4}$$

where l is the side length of the equilateral triangle, and a_i ($i = 1$, 2, or 3) is the pile-up width on three sides of the

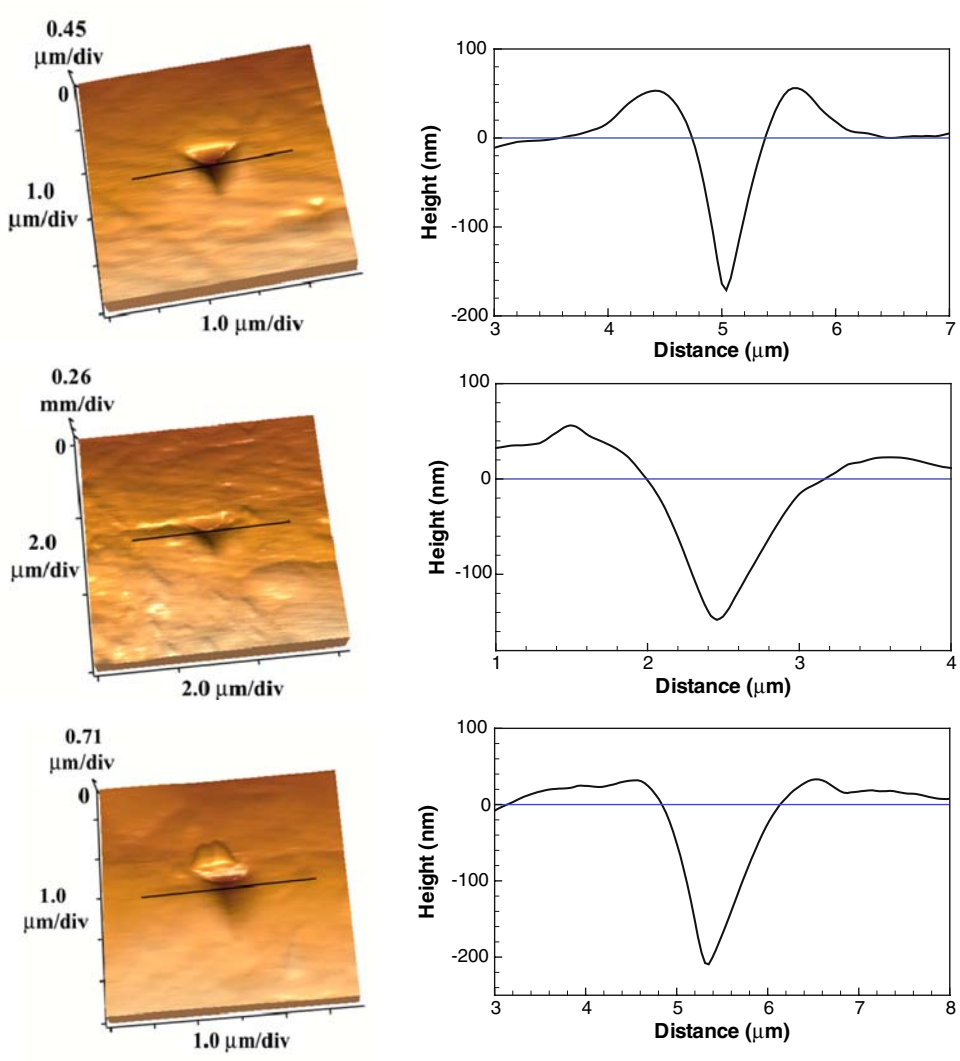

Fig. 5 Scanning probe microscopy images with scan line across indent on Au, $AuIn_2$ (annealed for 40 min), and In, and their corresponding scan profiles

Berkovich indent. The pile-up width a_i is determined using the scan line profile from each indent. It is defined as the horizontal distance between the pile-up contact perimeter and the edge of the indentation, which is illustrated in Fig. 6 for an indent on bulk gold with a maximum load of 800 μN. The side length of the equilateral triangle, l, is calculated through the calculation of contact area. The equilateral triangular contact area created from the three side pyramidal indenter can be calculated by:

$$A_c = \frac{l^2}{4}\tan 60^\circ = 0.433l^2. \quad (5)$$

For a cube corner tip, similar method can be applied to correct the contact area. From the tip area function for cube corner tip, the contact area can also be obtained as:

$$A_c = 2.598h_c^2. \quad (6)$$

By combining Eqs. 5 and 6, the side length of the equilateral triangle, l, can be represented by

$$l = 2.449h_c. \quad (7)$$

Combing Eqs. 4 and 7, the modified true contact area is represented by

$$A = A_{O-P} + A_{PU} = A_{O-P} + 1.922h_c \sum a_i, \quad (8)$$

where A_{O-P} is the original contact area obtained using Oliver and Pharr method. By using Eq. 8, contact areas were modified on each indent of the three materials, and the results show that the average modified contact area increases by 51.6% of the original contact area in gold, 39.5% in indium, 38.7% in $AuIn_2$ annealed for 10 min, 27.2% in $AuIn_2$ annealed for 40 min, and 33.7% in $AuIn_2$ annealed for 120 min.

By correcting the contact area, Fig. 7 shows a comparison of the reduced modulus and hardness of gold, indium, and the IMC $AuIn_2$ before and after the pile-up correction. It is calculated that gold has the greatest pile-up effect on its mechanical properties. After correction of the contact

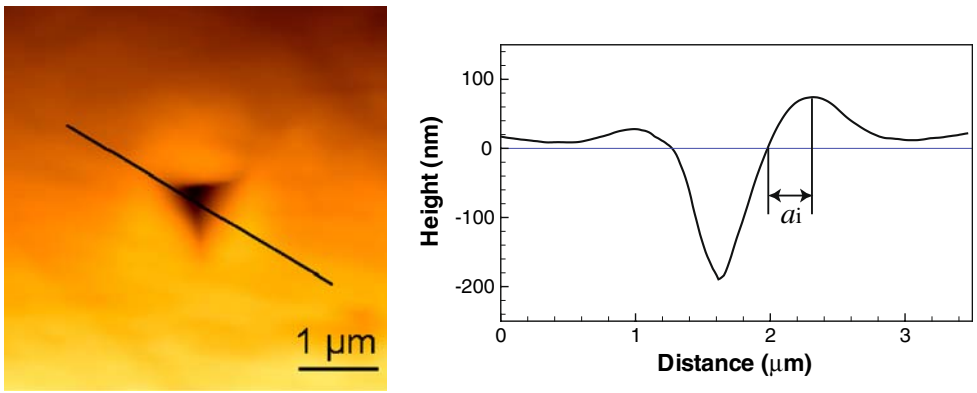

Fig. 6 Scanning probe microscopy images with scan line across indent on Au and its corresponding scan profile, which illustrates the calculation of modified contact area

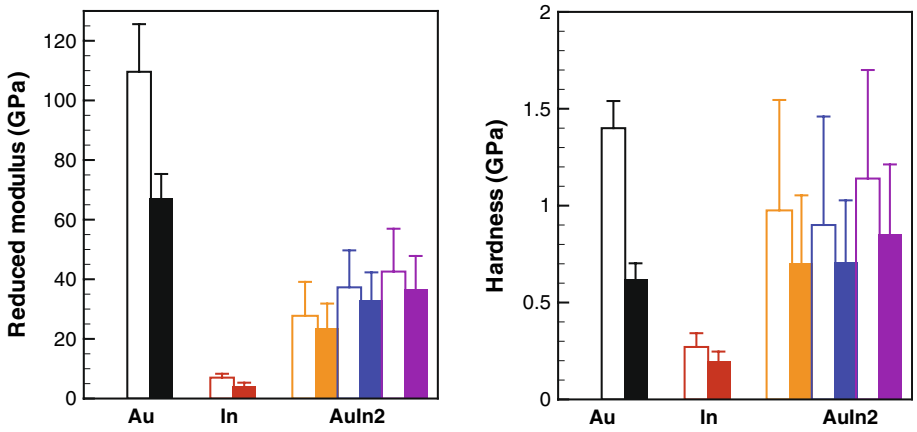

Fig. 7 Comparison of reduced modulus and hardness of Au, In, and $AuIn_2$ (*left to right*: annealing time of 10, 40, and 120 min) from calculations before and after the correction of contact area due to pile-up effect. The *hollow bar* represents original reduced modulus and hardness based on standard Oliver and Pharr method, and *solid bar* represents corrected reduced modulus and hardness from pile-up

area, for gold the reduced modulus decreased 18.7%, and hardness decreased 34.0%. For indium, the reduced modulus decreased 15.3%, and hardness decreased 28.3%. For $AuIn_2$ annealed for 10 min, the reduced modulus decreased 14.5%, and hardness decreased 27.9%. For $AuIn_2$ annealed for 40 min, the reduced modulus decreased 11.3%, and hardness decreased 21.4%. For $AuIn_2$ annealed for 120 min, the reduced modulus decreased 13.5%, and hardness decreased 25.2%. From Fig. 7, it can also be concluded that the reduced modulus and hardness of $AuIn_2$ are both much higher than those of indium. Especially, the hardness of $AuIn_2$ is 0.70 GPa for the sample annealed for 10 min, 0.71 GPa for sample annealed for 40 min, and 0.86 GPa for sample annealed for 120 min. These hardness values are either close to or slightly greater than that of gold of 0.62 GPa. This clearly supports that the $AuIn_2$ formation strengthens the indium matrix. Comparing mechanical properties of $AuIn_2$ annealed for 10, 40, and 120 min, one can observe a clear increase in reduced modulus and a slight increase in hardness with increasing annealing time. It is well-known that elastic modulus is an intrinsic material property, and it is a measure of the atomic bond strength. Materials with stronger atomic bonds always have a higher elastic modulus [20]. When annealing the materials, with increasing annealing time, more interactions will take place between gold and indium, thus forming a stronger atomic bond in their IMC $AuIn_2$. This explains the great increase of elastic modulus of $AuIn_2$ with increasing annealing time. Furthermore, it has been suggested that the mechanical hardness (H) of materials is related to their Young's modulus (E) by the relationship of $H = \alpha\beta E$, where β is a scaling factor for the mechanical hardness of an indented solid, and α is a fitted constant [20]. This explains why the hardness has a different degree of increase with increasing annealing time.

In addition to the correction of the contact area due to pile-up, it is necessary to interpret the relation between the pile-up degree and materials plastic properties. From several nanoindentation experiments and computational modeling, it is found that the degree of pile-up is dependent on the ratio of Young's modulus over yield strength E/σ_y and the work hardening behavior. The degree of pile-up is greatest in materials with high E/σ_y and lowest or no capacity for work hardening materials. Furthermore, Bolshakova and Pharr [21] found a unique correlation between E/σ_y and the experimentally measurable ratio of final indentation depth h_f over maximum indentation depth h_{max}. They found that pile-up is significant only when h_f/h_{max} is greater than 0.7 and the material does not appreciably work harden. When h_f/h_{max} is less than 0.7, or materials

moderately work harden, pile-up is not a significant factor. In this study, h_f/h_{max} was calculated based on the direct measurement from nanoindentation and averaged over each indent of three materials. The average value of h_f/h_{max} is 0.96 for gold, 0.86 for indium, 0.89 for $AuIn_2$ annealed for 10 min, 0.87 for $AuIn_2$ anneal for 40 min, and 0.9 for $AuIn_2$ annealed for 120 min. The higher value of h_f/h_{max} in gold indicates a greater degree of pile-up, which confirms the observation from the scan line profile as shown in Fig. 5.

Discussions and conclusions

In this study, gold and indium IMCs formation for low temperature solder bonding was investigated by imbedding a gold wire into an annealing indium solder. A low annealing temperature of 160 °C was applied, which is just above the melting temperature of indium at 156 °C. $AuIn_2$ precipitates were confirmed to be predominately formed in the IMCs by XRD. Different annealing times of 10, 40, and 120 min were applied to study the stabilization time of $AuIn_2$. With thermal considerations, $AuIn_2$ was confirmed to be formed at an annealing temperature as low as 160 °C, and with annealing times ranging from 10 to 120 min. In addition, the microstructure of the interfacial region of the gold wire with indium solder was investigated by SEM. The mechanical behavior of gold, indium, and their IMCs with different annealing times were studied by nanoindentation. Due to the pile-up effect, the contact area of indent on all materials were corrected based on an extended semi-ellipse model for cube corner indenter tip, and the mechanical properties including reduced modulus and hardness were calculated based on the corrected contact area. Furthermore, the pile-up degree was analyzed by the ratio of final indentation depth over the maximum indentation depth h_f/h_{max}, which is dependent on the important pile-up factor $E/\sigma y$. Gold was observed to have the greatest degree of pile-up, and this can be explained well from its highest value of h_f/h_{max}. The reduced modulus and hardness measured from nanoindentation indicate a significant strengthening of the indium solder by the $AuIn_2$ nanoparticles. Increase of reduced modulus and hardness with increasing annealing time is mainly due to the strengthening of the atomic bonding in the IMCs.

In conclusion, indium solder strength can be greatly enhanced by forming an intermetallic bonding of $AuIn_2$. On the other hand, the stable form of IMC $AuIn_2$ can be formed from a liquid–solid reaction of gold and indium with a low annealing temperature of 160 °C, and with a wide range of annealing times from 10 to 120 min. Furthermore, the mechanical properties including elastic modulus and hardness were enhanced by increasing the annealing time.

Acknowledgement J. Lian and J. Wang acknowledge the financial support from the University of California Academic Senate and the University of Washington Regents.

References

1. De Moor P (2008) Nucl Instrum Methods Phys Res A 591:224
2. Ho PS, Wang G, Ding M, Zhao J-H, Dai X (2004) Microelectron Reliab 44:719
3. Nah J-W, Kim JH, Lee HM, Paik K-W (2004) Acta Mater 52:129
4. Yeo A, Ebersberger B, Lee C (2008) Microelectron Reliab 48:1847
5. Liu YM, Chuang TH (2000) J Electron Mater 29:405
6. Peng C-T, Kuo C-T, Chiang K-N, Ku T, Chang K (2006) Microelectron Reliab 46:523
7. Laurila T, Vuorinen V, Kivilahti JK (2005) Mater Sci Eng R Rep 49:1
8. Simic V, Marinkovic Z (1977) Thin Solid Films 41:57
9. Kuhmann JF, Maly K, Preuss A, Adolphi B, Drescher K, Wirth T, Oesterle W, Fanciulli M, Weyer G (1998) J Electrochem Soc 145:2138
10. Matijasevic GS, Lee CC, Wang CY (1993) Thin Solid Films 223:276
11. Wang TB, Shen ZZ, Ye RQ, Xie XM, Stubhan F, Freytag J (2000) J Electron Mater 29:443
12. Chromik R, Vinci R, Allen S, Notis M (2003) J Miner Met Mater Soc 55:66
13. Deng X, Chawla N, Chawla KK, Koopman M (2004) Acta Mater 52:4291
14. Xu L, Pang JHL (2006) Thin Solid Films 504:362
15. Hlava P (2006) Microsc Microanal 12:1072
16. So WW, Lee CC (2000) IEEE Trans Compon Packag Technol 23:377
17. Oliver WC, Pharr GM (1992) J Mater Res 7:1564
18. Li X, Bhushan B (2002) Mater Charact 48:11
19. Kese KO, Li ZC, Bergman B (2004) J Mater Res 19:3109
20. Clerc DG, Ledbetter HM (1998) J Phys Chem Solids 59:1071
21. Bolshakov A, Pharr GM (1998) J Mater Res 13:1049